Arf6 promotes autophagosome formation via effects on phosphatidylinositol 4,5-bisphosphate and phospholipase D

Kevin Moreau, Brinda Ravikumar, Claudia Puri, and David C. Rubinsztein

Department of Medical Genetics, Cambridge Institute for Medical Research, Cambridge CB2 0XY, England, UK

Macroautophagy (in this paper referred to as autophagy) and the ubiquitin–proteasome system are the two major catabolic systems in cells. Autophagy involves sequestration of cytosolic contents in double membrane–bounded vesicles called autophagosomes. The membrane source for autophagosomes has received much attention, and diverse sources, such as the plasma membrane, Golgi, endoplasmic reticulum, and mitochondria, have been implicated. These may not be mutually exclusive, but the exact sources and mechanism involved in the formation of autophagosomes are still unclear. In this paper, we identify a positive role for the small G protein Arf6 in autophagosome formation. The effect of Arf6 on autophagy is mediated by its role in the generation of phosphatidylinositol 4,5-bisphosphate (PIP_2) and in inducing phospholipase D (PLD) activity. PIP_2 and PLD may themselves promote autophagosome biogenesis by influencing endocytic uptake of plasma membrane into autophagosome precursors. However, Arf6 may also influence autophagy by indirect effects, such as either by regulating membrane flow from other compartments or by modulating PLD activity independently of the mammalian target of rapamycin.

Introduction

Autophagy, one of the major cellular degradation machineries, involves the engulfment of cytoplasmic content by double-membraned vesicles called autophagosomes, which transport the materials to be degraded to lysosomes, where they are degraded. The process of autophagy begins with the formation of distinct structures called preautophagic structures (PASs) or phagophores, which extend and fuse to form the autophagosome (Xie and Klionsky, 2007; Mizushima et al., 2008; Ravikumar et al., 2009). Several highly conserved autophagy (Atg) proteins that function at key steps in the autophagy process have been identified. For example, Atg5, Atg12, and Atg16L1 form a large tetrameric complex involved in the initiation step, whereas phosphatidylethanolamine-conjugated Atg8/LC3 (LC3-II) is involved in the elongation and fusion steps of autophagosome formation (Xie and Klionsky, 2007; Mizushima et al., 2008; Ravikumar et al., 2009, 2010c). Consistent with this, the Atg12-Atg5–Atg16L1 complex decorates the PAS and dissociates after completion of autophagosome formation, whereas LC3-II is localized to both the PAS and fully formed autophagosomes. LC3-II is specifically targeted to autophagosomal membranes and strongly correlates with autophagosome number (Kabeya et al., 2000; Klionsky et al., 2008). To assess whether LC3-II formation is altered by a perturbation, one can assess its level in the presence of bafilomycin A1 (Baf A1), which inhibits LC3-II degradation by blocking autophagosome–lysosome fusion (Klionsky et al., 2008; Rubinsztein et al., 2009). Therefore, differences in LC3-II levels in response to particular conditions (siRNA and drug treatment) in the presence of Baf A1 reflect changes in autophagosome synthesis. The initiation step in the autophagy process is highly regulated, involving key signaling molecules, which function as a macromolecular complex, the best characterized being the Beclin 1–Vps34 and the Ulk1–mammalian

K. Moreau and B. Ravikumar contributed equally to this paper.

Correspondence to David C. Rubinsztein: dcr1000@hermes.cam.ac.uk

Abbreviations used in this paper: 5ase, 5-phosphatase; Arf, ADP ribosylation factor; ARNO, Arf nucleotide binding site opener; Baf A1, bafilomycin A1; CTX, cholera toxin; FKBP, FK506-binding protein; FRB, FKBP12-rapamycin binding; GEEC, GPi-enriched endocytic compartment; GPi, glycosylphosphatidylinositol; MEF, mouse embryonic fibroblast; MHC, major histocompatibility complex; mRFP, monomeric RFP; mTOR, mammalian target of rapamycin; PAS, preautophagic structure; PH, pleckstrin homology; PIP_2, phosphatidylinositol 4,5-bisphosphate; PIP5K, phosphatidylinositol 4-phosphate 5-kinase.

The Rockefeller University Press $30.00
J. Cell Biol. Vol. 196 No. 4 483–496
www.jcb.org/cgi/doi/10.1083/jcb.201110114

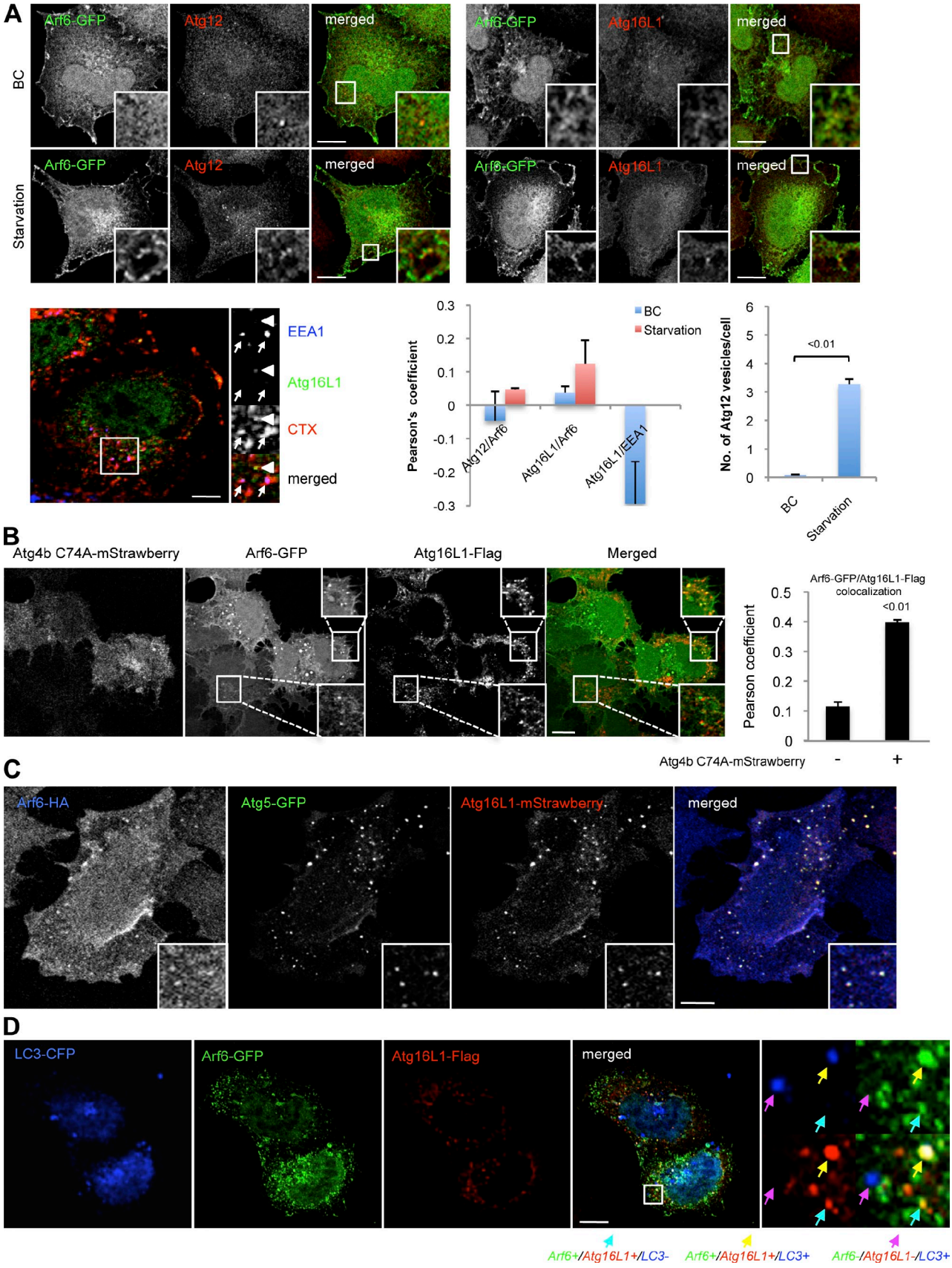

Figure 1. **Arf6 colocalizes with early autophagic markers.** (A) Colocalization between Arf6-GFP and endogenous Atg12 and Atg16L1. HeLa cells transiently expressing Arf6-GFP for 20 h were cultured in basal conditions (BC) or amino acid and serum starvation medium for 1 h. Cells were fixed and subjected to immunofluorescence with anti-Atg12 or anti-Atg16L1 antibodies. Confocal images of Arf6-GFP and either Atg12 or Atg16L1 are shown. A confocal image of Atg16L1, EEA1, and CTX subunit B conjugated to Alexa Fluor 555 (CTX; 20 min after internalization) is also shown at the bottom left.

target of rapamycin (mTOR) complexes (Xie and Klionsky, 2007; Mizushima et al., 2008; Ravikumar et al., 2009). However, the exact sequence of events involved in the formation of new autophagosomes is still unclear.

The membrane source for autophagosome biogenesis has received great attention recently, and diverse sources, such as plasma membrane, Golgi, endoplasmic reticulum, and mitochondria, have been implicated (Ylä-Anttila et al., 2009; Hailey et al., 2010; Hayashi-Nishino et al., 2010; Ravikumar et al., 2010a; van der Vaart et al., 2010; Yen et al., 2010). We recently demonstrated that clathrin-mediated endocytosis contributes membrane to Atg16L1-positive vesicles (LC3 negative), which mature to form phagophores (Atg16L1 positive and LC3 positive) and, subsequently, autophagosomes (Atg16L1 negative and LC3 positive; Ravikumar et al., 2010a,b). We showed that clathrin-dependent endocytosis is required both for the formation of autophagosomes, via the formation of Atg16L1-positive vesicles, and also for maturation of autophagosomes when early or late endosomes fuse with Atg16L1-negative, but LC3-positive, autophagosomes to form amphisomes. It is quite possible that vesicles from multiple membrane sources may contribute to autophagosomes and that these may fuse before autophagosome completion. Such fusion is a possibility, as we have observed homotypic fusion of Atg16L1-containing structures (Moreau et al., 2011). Understanding the regulation of membrane delivery from the plasma membrane to early autophagic structures will be important, as this is one of the initiating events in autophagosome biogenesis.

Here, we have identified a new role in autophagy for Arf6, an ADP ribosylation factor (Arf) family small G protein that is localized to the plasma membrane and the endocytic system (Donaldson, 2003; D'Souza-Schorey and Chavrier, 2006). Similar to other Arfs, Arf6 cycles between GTP-bound active and GDP-bound inactive forms. Arf6 stimulates phosphatidylinositol 4-phosphate 5-kinase (PIP5K) at the plasma membrane, which results in the generation of phosphatidylinositol 4,5-bisphosphate (PIP_2; Honda et al., 1999; Brown et al., 2001), an important second messenger that regulates membrane structure and function (Di Paolo and De Camilli, 2006; Doherty and McMahon, 2009). We find that Atg16L1-positive vesicles are associated with Arf6, which regulates autophagosome formation. This effect of Arf6 could be explained by its effects on plasma membrane PIP_2 production. Plasma membrane depletion of PIP_2 inhibited autophagy by blocking membrane delivery to autophagic precursors. Moreover, we identified GRAF1, a PIP_2-binding protein involved in clathrin-independent endocytosis via the glycosylphosphatidylinositol (GPi)-enriched endocytic compartments (GEECs) as a positive regulator of autophagosome formation, suggesting a clathrin-independent route for the biogenesis of autophagosomes. Our data suggest that Arf6 may also regulate autophagosome biogenesis by influencing PLD activity.

Results

Arf6 partially colocalizes with early autophagic markers

To understand the role of Arf6 in autophagy, we first examined the colocalization of Arf6-GFP with the endogenous phagophore proteins Atg12 and Atg16L1 by confocal microscopy. A previous study has shown that overexpressed Arf6 has the same distribution as endogenous Arf6 (Song et al., 1998). We have had to use overexpressed Arf6 in these experiments, as our mouse anti-Arf6 antibody, while working well on Western blots, does not give specific signals with immunocytochemistry (unpublished data), and rabbit antibodies would preclude colocalization analyses with the autophagy proteins in which we have used rabbit antibodies. We observed that Arf6-GFP partially colocalized with the phagophore proteins Atg12 and Atg16L1. This colocalization was enhanced by amino acid and serum starvation, which induce autophagosome formation (Fig. 1 A). We confirmed that Atg16L1 does not colocalize with EEA1, an early endosomal marker, but colocalizes well with internalized cholera toxin (CTX; which initially binds the plasma membrane), suggesting that an Atg16L1 vesicle is not an early endosome (Fig. 1 A; Ravikumar et al., 2010a,b). Arf6 also colocalized with exogenous Atg16L1 (Atg16L1-Flag; Fig. 1 B), and the colocalization was further enhanced in the presence of the Atg4B mutant (Atg4B C74A), which results in the accumulation of PASs by inhibiting LC3 processing (Fig. 1 B; Fujita et al., 2008). To confirm that the localization of Arf6 on Atg16L1 vesicles represented autophagic structures, we performed a triple colocalization analysis between Arf6, Atg16L1, and Atg5 (another autophagic precursor marker). We observed that Arf6 colocalized with Atg16L1 and Atg5 on the same vesicle (Fig. 1 C), confirming the autophagic nature of the vesicle. It is worth noting that Atg16L1-mStrawberry and Atg5-GFP colocalized almost perfectly (Fig. 1 C), indicating that the Atg16L1 vesicles formed by exogenous expression of Atg16L1-mStrawberry were indeed early autophagic structures, as already shown for Atg16L1-Flag (Ravikumar et al., 2010a). Furthermore, Arf6 localized on Atg16L1-positive/LC3-negative vesicles (Fig. 1 D, blue arrows) and Atg16L1-positive/LC3-positive vesicles (Fig. 1 D, yellow arrows) but

Please note that Atg16L1 does colocalize with CTX but not with EEA1. Arrows indicate colocalization between EEA1 and cholera toxin (CTX) but not with Atg16L1, whereas arrowheads indicate colocalization between Atg16L1 and CTX but not with EEA1. The Pearson's coefficient between Arf6 and either Atg12 or Atg16L1 is shown. $n = 50$ cells. Graph at the bottom right represents the number of Atg12 vesicles per cell under basal or amino acid and serum starvation for 1 h obtained using an automatic microscope. (B) HeLa cells transiently expressing Atg4B C74A–mStrawberry, Arf6-GFP, and Atg16L1-Flag (red) for 20 h were fixed and subjected to immunofluorescence with the anti-Flag antibody. Confocal images of Atg4B C74A–mStrawberry, Arf6-GFP (green), and Atg16L1-Flag (red) are shown. The colocalization (Pearson's coefficient) between Atg16L1-Flag and Arf6-GFP is shown. $n = 20$ cells. (C) HeLa cells transiently expressing Atg5-GFP, Arf6-HA, and Atg16L1-mStrawberry for 20 h were fixed and subjected to immunofluorescence with the anti-HA antibody. Confocal images of Atg5-GFP, Arf6-HA, and Atg16L1-mStrawberry are shown. (D) HeLa cells transiently expressing LC3-CFP, Arf6-GFP, and Atg16L1-Flag for 20 h were fixed and subjected to immunofluorescence with the anti-Flag antibody. Confocal images of LC3-CFP, Arf6-GFP, and Atg16L1-Flag are shown. Higher magnifications of the colocalizations are shown in the insets. The data are means ± SD. Bars, 5 µm.

not on Atg16L1-negative/LC3-positive vesicles (Fig. 1 D, purple arrows), indicating that Arf6 is localized on early autophagic structures and suggesting that Arf6 is released from completed autophagosomes (Fig. 1 D). Arf6 levels appeared to be upregulated upon starvation, and this correlated with autophagic induction as seen by Western blotting for Arf6 and LC3-II in mouse embryonic fibroblasts (MEFs) cultured in rich conditions or amino acid and serum starved for 1 h (Fig. S1 A).

Arf6 regulates phagophore formation

Arf6 undergoes a cycle of GTP binding and hydrolysis to form the GTP-bound active and GDP-bound inactive forms of the protein. Expression of Arf6 Q67L, a GTP hydrolysis-resistant mutant, leads to the accumulation of PIP_2-positive actin-coated vacuoles that are unable to recycle membrane back to the plasma membrane (Brown et al., 2001; D'Souza-Schorey and Chavrier, 2006). We observed that although Arf6-GFP colocalized with Atg16L1-Flag, Arf6 Q67L did not, indicating that Atg16L1 is not present in these previously described internal vacuoles (Fig. 2 A). We next studied the effect of Arf6 on the formation of Atg16L1, Atg12, and LC3 vesicles under basal conditions or amino acid and serum starvation (Figs. 2 B and S1, B–D), using transient expression of Arf6 Q67L as the constitutively active form compared with wild-type Arf6 or empty vector, and used siRNA against Arf6 to inhibit its function. We used the siRNA method instead of the dominant-negative form of Arf6 (Arf6 T27N) because of the controversial data obtained with this mutant (Macia et al., 2004). Transient expression of Arf6 Q67L dramatically decreased the formation of Atg16L1-mStrawberry vesicles under both basal conditions and amino acid and serum starvation (Fig. S1 C). The number of endogenous LC3 vesicles also decreased in Arf6 Q67L–expressing cells compared with Arf6 wild type– or empty vector–expressing cells (Fig. S1 D). To confirm that Arf6 Q67L decreased the formation of phagophores, we scored the number of endogenous Atg12 vesicles in Atg4B mutant (Atg4B C74A)–expressing cells under both basal conditions and amino acid and serum starvation (Fig. 2 B). In Atg4B mutant–expressing cells, we observed that transient expression of Arf6 Q67L decreased the number of Atg12 vesicles compared with wild-type Arf6 or empty vector (Fig. 2 B), confirming that Arf6 Q67L blocked the formation of early autophagic structures. The number of Atg16L1-GFP vesicles or endogenous Atg12 vesicles decreased in Arf6 knockdown cells compared with the control (Fig. 2 C). These data together indicated that Arf6 plays a major role in the formation of early autophagic vesicles. We confirmed that the regulation of autophagy by Arf6 is not confined to HeLa cells by showing that transient expression of Arf6 Q67L in CHO cells decreased the formation of Atg16L1-mStrawberry compared with wild-type Arf6 or empty vector (Fig. S1 E).

Arf6 regulates autophagosome formation independently of mTOR

To confirm the role of Arf6 in autophagosome formation, we examined the key autophagosomal marker LC3-II by Western blotting. Arf6 knockdown reduced LC3-II levels in both untreated and Baf A1–treated cells under basal- or autophagy-induced conditions (starvation or trehalose conditions; Figs. 3 A and S2 A). These effects were not the consequence of potential off-target effects of the siRNAs because single siRNAs against Arf6, which efficiently knock down Arf6 (number 1, 2, and 4), decreased LC3-II with or without Baf A1, in contrast to siRNA number 3, which did not effectively knock down Arf6 (Fig. 3 B). We confirmed the defect in autophagosome formation when Arf6 is inhibited using another autophagy assay, a GFP–monomeric RFP (mRFP)–LC3 expression construct that allows discrimination between early autophagic organelles (GFP positive/mRFP positive) and acidified autolysosomes (GFP negative/mRFP positive), as the GFP signal (but not the mRFP) is quenched inside acidic compartments (Kimura et al., 2007). In cells stably expressing GFP-mRFP-LC3, we observed a decrease in LC3 vesicle number (total autophagic vesicles, autophagosomes, and autolysosomes) in Arf6 knockdown cells compared with controls (Fig. S2 B). Arf6 knockdown increased the level of p62, an endogenous autophagy substrate, in basal or amino acid and serum starvation conditions (Fig. S2 C). These data demonstrate a role of Arf6 in autophagosome formation.

To understand the mechanism by which Arf6 regulates autophagy, we first checked the effect of Arf6 knockdown on mTOR activation, a negative regulator of autophagy, by measuring the phosphorylation of one of its downstream targets, p70S6 kinase (Ravikumar et al., 2010c). Arf6 knockdown decreased p70S6 kinase phosphorylation, suggesting that Arf6 regulates autophagy independently of mTOR because mTOR inhibition should lead to autophagy induction (Ravikumar et al., 2010c), and we observed an autophagy inhibition in Arf6 knockdown cells (Fig. S2 D). We next tested whether Arf6 activation mediated by the exchange of GDP with GTP was required for autophagosome formation. We observed that Arf nucleotide binding site opener (ARNO; cytohesin-2) knockdown, a guanine nucleotide exchange factor localized at the plasma membrane that increases the rate of exchange of bound GDP with GTP on Arf6 (Donaldson, 2003; D'Souza-Schorey and Chavrier, 2006), decreased LC3-II levels in Baf A1–treated cells under basal conditions or amino acid and serum starvation (Fig. 3 C).

PIP_2 regulates autophagosome formation

Arf6 regulates the formation of PIP_2 at the plasma membrane via its effect on PIP5K (Honda et al., 1999; Brown et al., 2001). AP-2 can interact with PIP_2, and the generation of PIP_2 can lead to changes in membrane curvature, suggesting that PIP_2 may be a key factor initiating the budding events at the plasma membrane that affects autophagosome formation from the plasma membrane as we recently proposed (Ravikumar et al., 2010a). We therefore examined the role of PIP_2 in autophagy. We studied the localization of PIP_2 using a construct encoding the pleckstrin homology (PH) domain of PLC-δ fused to GFP (PLC(PH)-GFP; Várnai and Balla, 1998). We observed that the endogenous phagophore proteins Atg16L1, Atg12, and Atg5 partially colocalized with PLC(PH)-GFP, correlating with data obtained with Arf6 colocalization (Fig. 4 A). The percentage of colocalization increased when we overexpressed Atg16L1-Flag (Fig. 4 B). Transient expression of Arf6 Q67L induced the localization of PIP_2 inside internal structures, correlating with an absence of Atg16L1

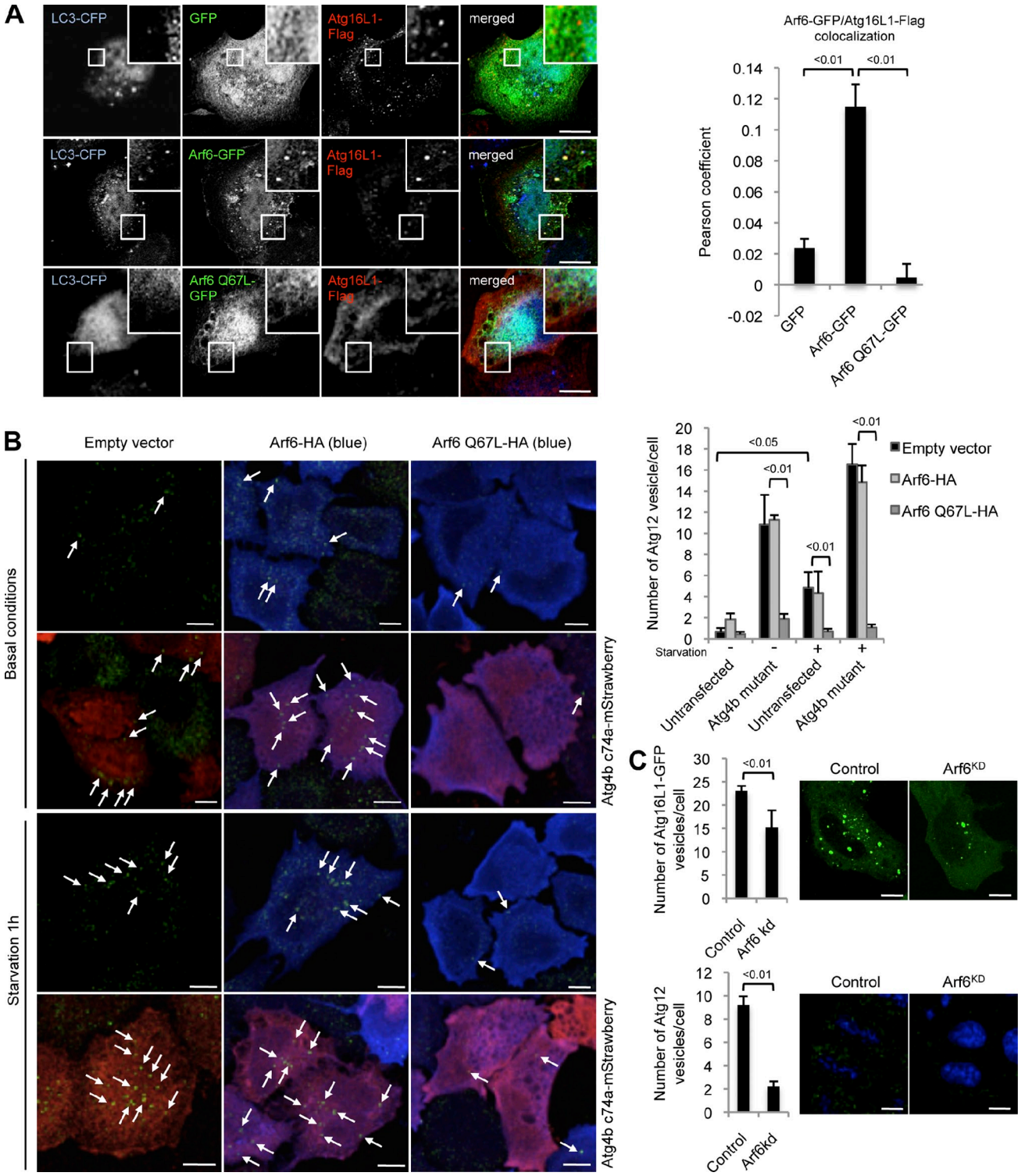

Figure 2. **Arf6 regulates phagophore formation.** (A) HeLa cells transiently expressing LC3-CFP, Atg16L1-Flag, and either GFP, Arf6-GFP, or Arf6 Q67L-GFP for 20 h were fixed and subjected to immunofluorescence with an anti-Flag antibody. Confocal images of LC3-CFP, Atg16L1-Flag, and either GFP, Arf6-GFP, or Arf6 Q67L-GFP are shown. Higher magnifications of the colocalizations are shown in the insets. The colocalization (Pearson's coefficient) between Atg16L1-Flag vesicles and either GFP, Arf6-GFP, or Arf6 Q67L-GFP is shown. For colocalization, the data are means ± SD. n = 20 cells. (B) HeLa cells transiently expressing Arf6-HA, Arf6 Q67L-HA, or an empty vector and Atg4B C74A–mStrawberry as indicated for 20 h were cultured in basal conditions or amino acid and serum starvation medium for 1 h. Cells were fixed and subjected to immunofluorescence with anti-Atg12 and anti-HA antibodies. Confocal images of Atg12 (green), Arf6, and Atg4B C74A–mStrawberry (red) are shown. The data represent the means ± SD of the number of Atg12 vesicles per cell obtained from three independent experiments in which ≥200 cells were analyzed. Please note that individual channels of the pictures are shown in Fig. S1 B. Arrows indicate Atg12 vesicles, which are larger and brighter than the background-staining speckles. (C) HeLa cells transfected with two rounds of control or Arf6 siRNA for 5 d were fixed and subjected to automatic counting of Atg16L1-GFP or endogenous Atg12 vesicles. Representative confocal pictures are shown. The data represent the means ± SD of the number of Atg16L1-GFP vesicles or Atg12 vesicles per cell obtained from three independent experiments in which ≥200 cells were analyzed. kd, knockdown. Bars, 5 µm.

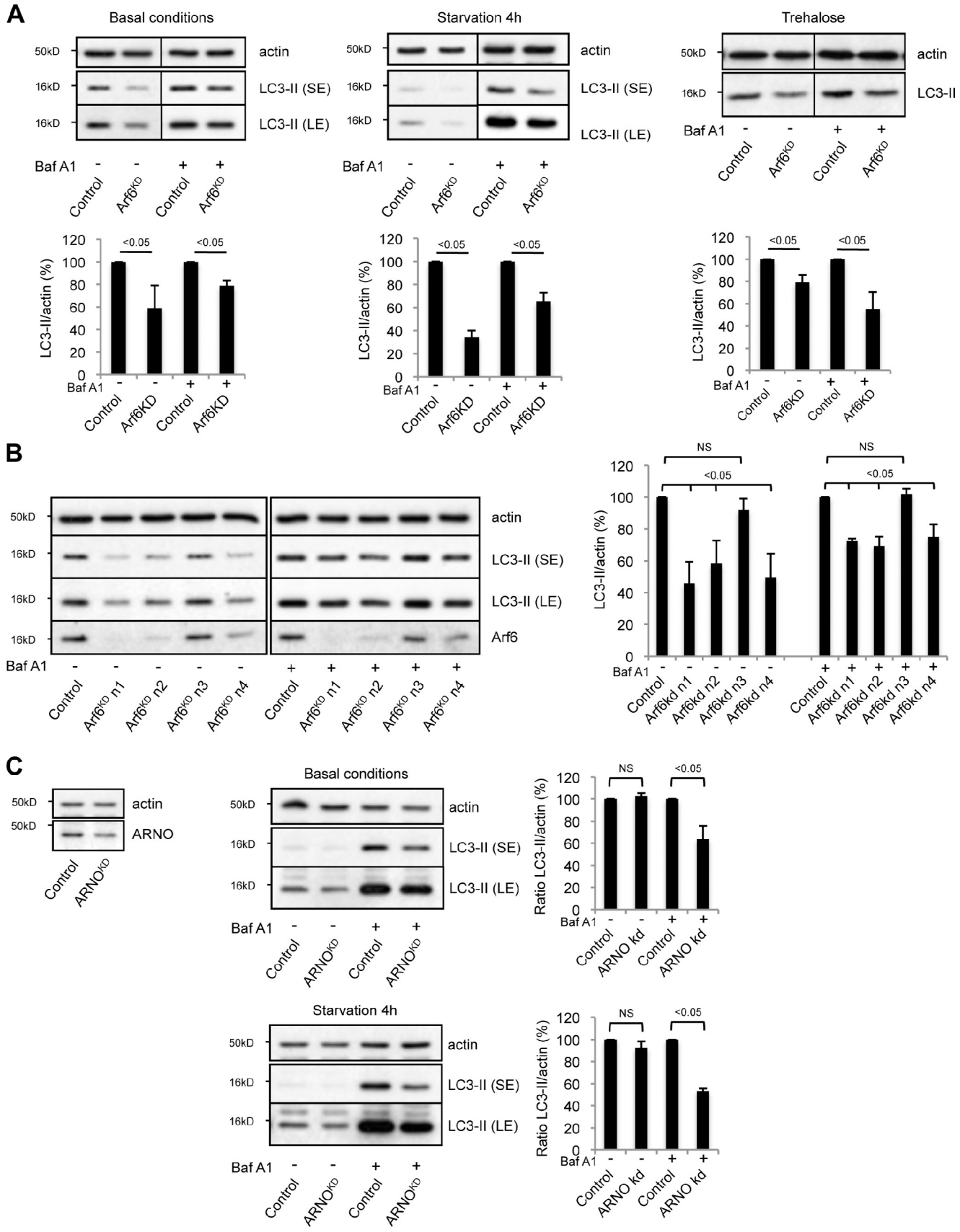

Figure 3. **Arf6 regulates autophagosome formation.** (A) HeLa cells transfected with two rounds of control or Arf6 siRNA for 5 d were cultured in basal conditions or in starvation medium for 4 h or treated with 100 mM trehalose for the last 20 h and with 400 nM bafilomycin A1 (Baf A1) as indicated for 4 h. Cells were lysed and subjected to Western blotting with the indicated antibodies. The data represent the means ± SD of the percentage of LC3-II/actin ratios obtained from three independent experiments. Black lines indicate that intervening lanes have been spliced out. (B) HeLa cells transfected with two

vesicles (Fig. 4 B). These data suggested that PIP_2 is localized to early autophagic vesicles in an Arf6-dependent fashion.

We acutely depleted PIP_2 at the plasma membrane using a heterodimerization system, which recruits an inositol 5-phosphatase (5ase; 5ase-mRFP) to the cell surface after addition of rapamycin (Fig. 4 C; Várnai et al., 2006; Zoncu et al., 2007, 2009). This technique has been previously shown to cause a massive block of endocytosis (Várnai et al., 2006; Zoncu et al., 2007, 2009). After recruitment of a control fusion protein (mRFP) with rapamycin treatment, LC3-II increased under Baf A1 treatment (which corresponded to the rapamycin effect on autophagy already described; Ravikumar et al., 2009), whereas LC3-II decreased after recruitment of the 5ase (Fig. 4 C). The recruitment of 5ase at the plasma membrane also decreased the formation of endogenous Atg12 vesicles (Fig. 4 D). These data indicated a role of plasma membrane PIP_2 in autophagy, more precisely in the formation of early autophagic precursors. To further confirm the role of PIP_2 in autophagosome formation, we knocked down PIP5K, an enzyme that generates PIP_2 (Honda et al., 1999). PIP5K knockdown decreased the level of LC3-II in Baf A1–treated cells, in basal- or autophagy-induced conditions resulting from amino acid and serum starvation (Fig. S3 A) and decreased the formation of Atg16L1-GFP vesicles (Fig. S3 B). In cells stably expressing GFP-mRFP-LC3, we observed a decrease in the LC3 vesicle number (total autophagic vesicles, autophagosomes, and autolysosomes) in PIP5K knockdown cells compared with controls (Fig. S3 C). We cannot exclude that other kinases, which regulate PIP_2 formation, influence autophagy (Rameh et al., 1997; Di Paolo and De Camilli, 2006).

PIP_2 conducts membrane delivery to Atg16L1 precursors

PIP_2 regulates endocytosis, in part, by influencing dynamin recruitment, which mediates endosomal scission (Di Paolo and De Camilli, 2006; Doherty and McMahon, 2009). Previously, we showed that clathrin-mediated endocytosis is required for Atg16L1 vesicle and autophagosome formation, which is associated with plasma membrane contributing to Atg16L1 structures (Ravikumar et al., 2010a). Internalization of plasma membrane was critical because blockage of endosomal scission by dynamin inhibition resulted in the accumulation of Atg16L1 at the plasma membrane and impairment of Atg16L1 vesicle formation (Ravikumar et al., 2010a). Accordingly, we hypothesized that PIP_2 regulated autophagy by influencing endocytosis. We observed that PIP_2 depletion, using the heterodimerization system that decreased Atg12 vesicle formation (Fig. 4 D), also decreased the colocalization of Atg16L1 with the endocytic tracer, CTX subunit B, which binds to the outside of the plasma membrane (Fig. 5, A and B). This is also seen when one perturbs clathrin-mediated endocytosis (Ravikumar et al., 2010a) or with knockdowns of either Arf6 or PIP5K (Fig. 5 C). Finally, PIP_2 depletion resulted in the formation of tubules labeled with CTX subunit B (Figs. 5 A and S3 D), which colocalized with plasma membrane marker (5ase–FK506- binding protein [FKBP]–mRFP when the cells were treated with rapamycin), suggesting these were endosomal intermediates that had failed to undergo scission, as would be predicted by PIP_2 depletion. Indeed, a similar phenotype was seen in cells treated with a dynamin inhibitor (Ravikumar et al., 2010a), consistent with a scission defect.

GRAF1, a PIP_2-binding protein, regulates autophagy

Arf6 regulates forms of clathrin-independent endocytosis (Donaldson et al., 2009). Accordingly, we tested whether a form of clathrin-independent endocytosis, the GEEC pathway, may be relevant to autophagosome formation. We considered this possibility because GRAF1, the first specific noncargo marker for GEEC is known to bind PIP_2 (Lundmark et al., 2008). Our hypothesis was strengthened when we observed that Atg16L1-Flag colocalized with GFP-tagged full-length GRAF1 (GRAF1-GFP) and GPi-mRFP or CTX in vesicular structures (Fig. S4 A). A previous study has shown that overexpressed GRAF1 has the same distribution as endogenous GRAF1 (Lundmark et al., 2008). We have had to use overexpressed GRAF1 in these experiments, as our rabbit anti-GRAF1 antibody, while working well on Western blots, does not give specific signals with immunocytochemistry (unpublished data). We also observed that overexpressed GFP-tagged GRAF1 BAR+PH protein (missing the GTPase-activating protein, proline-rich, and SH3 domains; GRAF1 BAR+PH-GFP), which labels static tubular membranes and acts in a dominant-negative manner to stabilize early endocytic tubules (Lundmark et al., 2008), colocalized with Atg16L1-Flag, GPi-mRFP, and CTX (Fig. S4 A).

To provide direct support for a role of GEEC-dependent autophagy, we perturbed this form of endocytosis by modulating the activities of GRAF1 (Kumari and Mayor, 2008; Lundmark et al., 2008; Doherty and McMahon, 2009). We inhibited GRAF1 expression using three different siRNAs (ARHGAP26, GRAF1a, and GRAF1b; Fig. 6 A). The different siRNAs against GRAF1 decreased the LC3-II levels in Baf A1–treated cells (Fig. 6 A). In cells stably expressing GFP-mRFP-LC3, we observed a decrease in the LC3 vesicle number (total autophagic vesicles, autophagosomes, and autolysosomes) in GRAF1 knockdown cells compared with controls (Fig. S4 B). Overexpression of GRAF1-GFP increased LC3-II levels in Baf A1–treated cells, in contrast to the dominant-negative form of GRAF1 (GRAF1 BAR+PH-GFP; Fig. 6 B). This data indicated that GRAF1 is a positive regulator of autophagy and suggested that other forms of endocytosis are involved in autophagosome formation. Indeed, GRAF1 knockdown reduced the colocalization of endocytosed CTX with Atg16L1 (Fig. S4 C), like we observed with perturbation of clathrin-mediated endocytosis (Ravikumar et al., 2010a).

rounds of control or single Arf6 siRNA (n1 to n4) for 5 d were cultured in presence of 400 nM Baf A1 as indicated for 4 h. Cells were lysed and subjected to Western blotting with the indicated antibodies. (C) HeLa cells transfected with two rounds of control or ARNO siRNA for 5 d were cultured in basal conditions or in amino acid and serum starvation medium for 4 h and treated with 400 nM Baf A1 as indicated for 4 h. Cells were lysed and subjected to Western blotting with the indicated antibodies. (B and C) The data represent the means ± SD of the percentage of LC3-II/actin ratios obtained from two independent experiments. SE, short exposure; LE, longer exposure; kd, knockdown.

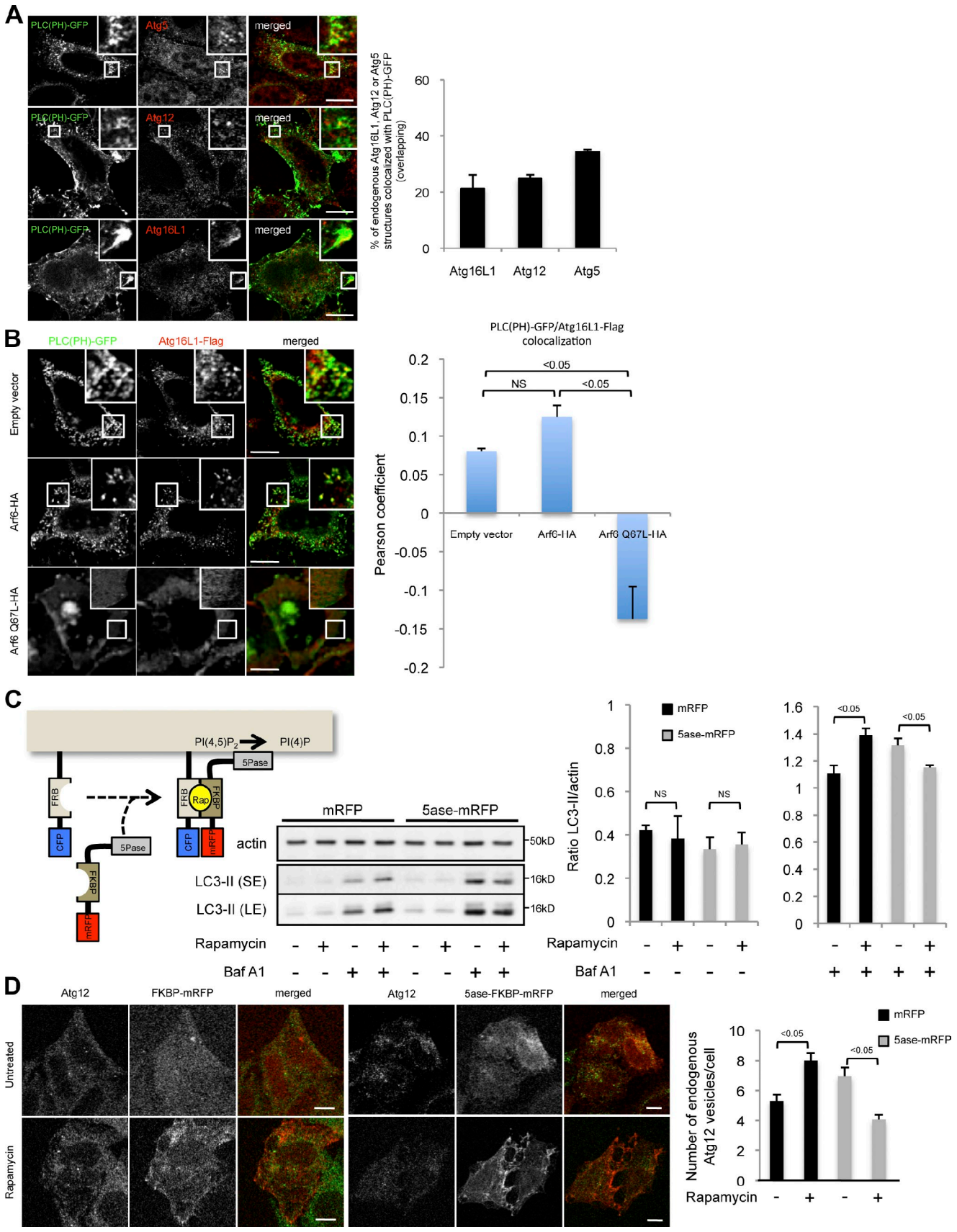

Figure 4. **PIP_2 regulates autophagosome formation.** (A) Colocalization between PLC(PH)-GFP and endogenous Atg5, Atg12, and Atg16L1. HeLa cells transiently expressing PLC(PH)-GFP for 20 h were cultured in starvation medium for 4 h. Cells were fixed and subjected to immunofluorescence with an anti-Atg5, anti-Atg12, or anti-Atg16L1 antibody. Confocal images of PLC(PH)-GFP and either Atg5, Atg12, or Atg16L1 are shown. The colocalization (overlapping) between PLC(PH)-GFP and Atg16L1-, Atg12-, or Atg5-positive vesicles is shown. (B) HeLa cells transiently expressing PLC(PH)-GFP, Atg16L1-Flag, and

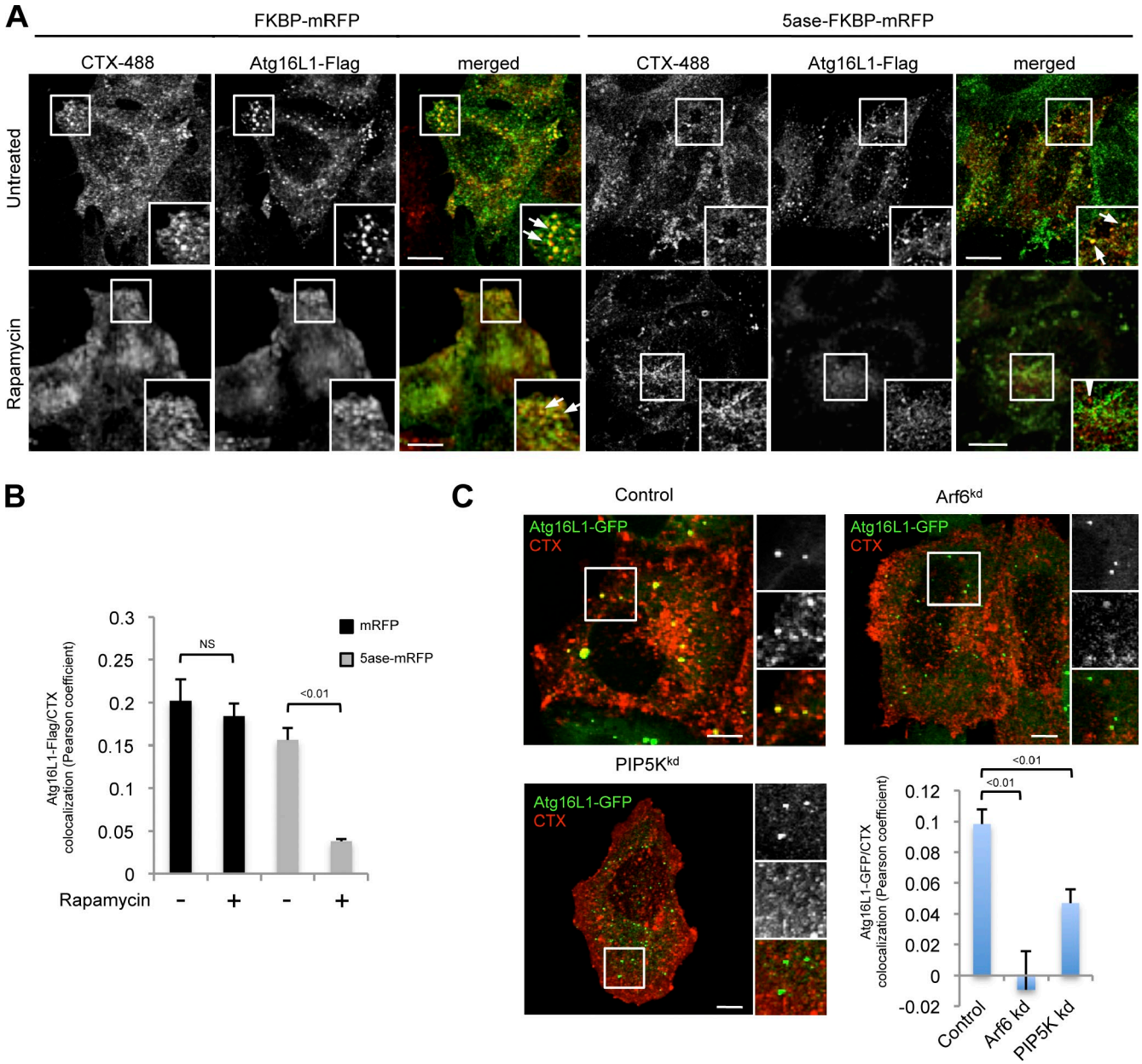

Figure 5. **PIP$_2$ conducts membrane delivery to Atg16L1 precursors.** (A) HeLa cells transiently expressing CFP-FRB and either mRFP-FKBP or mRFP-FKBP-5ase for 20 h were treated as indicated with 2.5 µM rapamycin and incubated for 30 min with CTX subunit B conjugated to Alexa Fluor 488 (CTX-488). Cells were fixed and subjected to confocal microscopy. Representative confocal pictures are shown. (B) The data represent the means ± SD of Atg16L1-CTX colocalization (Pearson's coefficient) from A. *n* > 30 cells for each condition. Arrows indicate Atg16L1-CTX colocalization, whereas the arrowhead indicates the absence of colocalization between Atg16L1 and CTX. (C) HeLa cells transfected with two rounds of control, Arf6, or PIP5K siRNA for 5 d were transfected during the last 20 h with Atg16L1-GFP. Cells were incubated for 30 min with CTX subunit B conjugated to Alexa Fluor 555 (CTX), fixed, and subjected to confocal microscopy analysis. The data represent the means ± SD of Atg16L1-CTX colocalization (Pearson's coefficient). *n* > 30 cells for each condition. Higher magnifications of the colocalizations are shown in the insets. kd, knockdown. Bars, 5 µm.

either Arf6-HA, Arf6 Q67L–HA, or an empty vector for 20 h were fixed and subjected to immunofluorescence with an anti-Flag antibody. Confocal images of PLC(PH)-GFP and Atg16L1-Flag are shown. The colocalization (Pearson's coefficient) between PLC(PH)-GFP and Atg16L1-Flag is shown. (A and B) For colocalization, the data are means ± SD. *n* = 20 cells. (C) HeLa cells transiently expressing CFP-FRB and either mRFP-FKBP or mRFP-FKBP-5ase for 20 h were treated as indicated with 2.5 µM rapamycin for 4 h and 400 nM bafilomycin A1 (Baf A1) for 4 h. Cells were lysed and subjected to Western blotting with the indicated antibodies. The data represent the means ± SD of the LC3-II/actin ratios obtained from three independent experiments. SE, short exposure; LE, longer exposure. (D) HeLa cells transiently expressing CFP-FRB and either mRFP-FKBP or mRFP-FKBP-5ase for 20 h were treated as indicated with 2.5 µM rapamycin for 1 h. Cells were fixed and subjected to confocal microscopy and to automatic counting of endogenous Atg12 vesicles. Representative confocal pictures are shown. The data represent the means ± SD of the number of endogenous Atg12 vesicles/cell obtained from three independent experiments. *n* = 500 cells in each experiment. Higher magnifications of the colocalizations are shown in the insets. Rap, rapamycin. Bars, 5 µm.

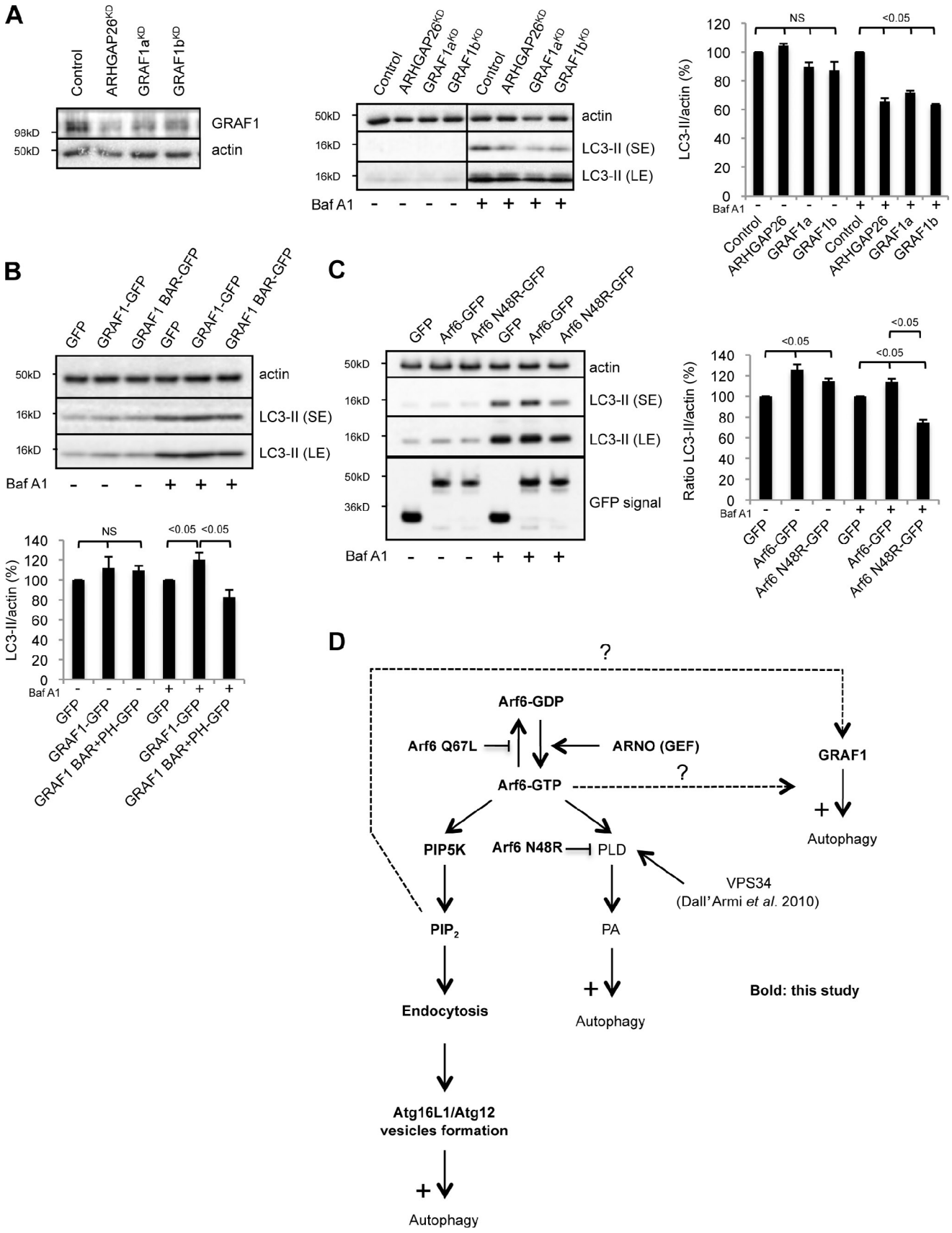

Figure 6. **GRAF1 is a positive regulator of autophagy.** (A) HeLa cells transfected with two rounds of control, ARHGAP26, GRAF1a, or GRAF1b siRNA for 5 d were treated with 400 nM bafilomycin A1 (Baf A1) as indicated for 4 h. Cells were lysed and subjected to Western blotting with the indicated antibodies. The data represent the means ± SD of the percentage of LC3-II/actin ratios obtained from three independent experiments. Black lines indicate that intervening lanes have been spliced out. (B) HeLa cells transiently expressing either GFP, GRAF1-GFP, or GRAF1 BAR+PH-GFP for 20 h were treated with

Atg16L1 does not positively affect Arf6 recycling, major histocompatibility complex (MHC) class I recycling, or clathrin-mediated endocytosis

Our data suggest that Arf6 regulates autophagosome formation via endocytosis regulation by modulating the pool of PIP_2 and that Arf6 activation is required for its activity on autophagy. In a reverse experiment, we studied whether autophagy regulated recycling of Arf6 or MHC class I, a specific cargo trafficking between the plasma membrane and the recycling endosome in an Arf6-dependent process (Donaldson, 2003; D'Souza-Schorey and Chavrier, 2006). Knockdowns of Atg16L1 or Atg9, which are both critical regulators of autophagosome formation, did not reduce either Arf6 or MHC class I recycling under basal conditions or amino acid and serum starvation (Fig. S5, A and B). In the same context, Atg16L1 knockdown did not influence either transferrin uptake or recycling as measured by flow cytometry (Fig. S5 C). To confirm this phenotype, we performed transferrin uptake and recycling experiments in Atg16L1-deficient MEFs. As observed in Atg16L1 knockdown cells, Atg16L1-deficient MEFs did not manifest any defect in transferrin recycling; transferrin uptake was slightly increased compared with wild-type background (Fig. S5 C). These data suggested that Atg16L1 does not positively regulate either clathrin-mediated endocytosis or Arf6 trafficking—if anything, Atg16L1 may slightly inhibit endocytosis. This does not influence our interpretations, and this interesting possibility will need further investigation in future studies.

Arf6 regulates autophagy via PLD activation

As Arf6 is involved in several different processes, we explored other possible mechanisms by which Arf6 regulated autophagy. We tested the role of PLD, a downstream target of Arf6, by blocking PLD activation using the Arf6 N48R mutant (Jovanovic et al., 2006). Arf6 N48R transient expression decreased LC3-II levels in Baf A1–treated cells, suggesting that PLD is a positive regulator of autophagy (Fig. 6 C). These data are consistent with recent data showing a positive role of PLD1 in autophagy (Dall'Armi et al., 2010).

Discussion

Arf6 gets activated and inactivated at many locations along the plasma membrane and regulates diverse cellular functions. Our study identifies a new role for Arf6 in autophagosome biogenesis. Arf6-dependent autophagosome formation requires the conformational changes between the GDP- and the GTP-bound forms of Arf6, as a mutant locked in the GTP form (Arf6 Q67L) or inhibition of GDP exchange to GTP (ARNO knockdown) blocked early stages of autophagy (Fig. 6 D). The identification of Arf6 and ARNO (cytohesin-2) as positive regulators of autophagy suggests that at least some of the regulation of autophagosome formation occurs at the plasma membrane because Arf6 and ARNO are mainly localized at this site (Donaldson, 2003; D'Souza-Schorey and Chavrier, 2006). This is consistent with our previous data showing uptake of plasma membrane into autophagosome precursors and autophagosomes via clathrin-mediated endocytosis. The functional relevance of this phenomenon was supported by the inhibition of Atg16L1 and LC3 vesicle formation by knockdowns of genes involved in clathrin-mediated endocytosis as well as experiments showing that short-term chemical and longer term genetic inhibition of vesicle scission caused accumulation of Atg16L1 at the plasma membrane, which was associated with decreased Atg16L1 vesicle formation (Ravikumar et al., 2010a).

The effects of Arf6 on autophagy correlate with its ability to regulate plasma membrane PIP_2 via PIP5K, adding autophagy to the growing list of functions regulated by PIP_2. Furthermore, the established requirement for this lipid in endocytosis (Di Paolo and De Camilli, 2006; Doherty and McMahon, 2009) is compatible with a role for this process in the formation of preautophagosomal structures (Ravikumar et al., 2010a). Depletion of PIP_2 or knockdowns of either Arf6 or PIP5K inhibited membrane delivery to early autophagic structures, similar to what we previously observed when clathrin-mediated endocytosis was inhibited (Fig. 6 D; Ravikumar et al., 2010a).

Regarding the pleiotropic effects of PIP_2 on several pathways, we cannot exclude that PIP_2 regulates autophagy via processes additional to clathrin-mediated endocytosis. We identified GRAF1, a PH and BAR domain protein involved in clathrin-independent endocytosis, which binds to PIP_2 as a positive regulator of autophagy (Kumari and Mayor, 2008; Lundmark et al., 2008; Doherty and McMahon, 2009). GRAF1 colocalized with early autophagic markers, and inhibition of its expression blocked membrane delivery to autophagic precursors (Fig. S4). It will be interesting to test whether Arf6 regulates GRAF1 recruitment to GEEC via PIP_2 (Fig. 6 D). This study suggests that different endocytosis pathways are involved in autophagosome formation.

In addition to affecting endocytic pathways regulating autophagosome biogenesis, Arf6 may also affect autophagy by indirect effects on other aspects in intracellular membrane flow. For instance, we found that Arf6 may influence autophagy by regulating PLD activity (Fig. 6 C). This result is consistent with a recent study showing a positive role of PLD1 in autophagy (Dall'Armi et al., 2010). Our data place Arf6 upstream to PLD in the regulation of autophagosome formation (Fig. 6 D).

400 nM Baf A1 as indicated for 4 h. Cells were lysed and subjected to Western blotting with the indicated antibodies. (C) HeLa cells transiently expressing either GFP, Arf6-GFP, or Arf6 N48R-GFP for 20 h were treated with 400 nM Baf A1 as indicated for 4 h. Cells were lysed and subjected to Western blotting with the indicated antibodies. (B and C) The data represent the means ± SD of the percentage of LC3-II/actin ratios obtained from two independent experiments. (D) Arf6 may regulate autophagy via multiple pathways: Arf6 activates PIP5K, which leads to the production of PIP_2 and the regulation of endocytosis; Arf6 activates PLD, which leads to the formation of phosphatidic acid (PA), a lipid involved in autophagosome formation. The question whether Arf6 regulates autophagy via GRAF1, a PIP_2-binding protein involved in clathrin-independent endocytosis, remains to be elucidated. Furthermore, Arf6 may regulate autophagy by affecting intracellular membrane flow via additional routes. SE, short exposure; LE, longer exposure.

Thus, Arf6 may coordinate autophagy via a few different pathways, suggesting that it is a critical regulator. In addition to the possible pathways we have characterized, we cannot exclude additional effects, including membrane availability via nonendocytic sources of autophagic membranes. However, our data suggest that Arf6 regulation of PIP_2 and PLD is an important function that impacts on autophagy.

Materials and methods

Cell culture

HeLa and CHO cells were cultured in DME D6546 (Invitrogen) containing 10% fetal bovine serum supplemented with 2 mM L-glutamine and 100 U/ml penicillin/streptomycin in 5% CO_2 at 37°C. Wild-type or Atg16L1-deficient MEFs were cultured in DME D6546 containing 10% fetal bovine serum supplemented with 2 mM L-glutamine and 100 U/ml penicillin/streptomycin in 5% CO_2 at 37°C. HeLa cells stably expressing the GFP-mRFP-LC3 protein were cultured in DME D6546 containing 10% fetal bovine serum supplemented with 2 mM L-glutamine, 100 U/ml penicillin/streptomycin and 500 µg/ml G418 (Sigma-Aldrich) in 5% CO_2 at 37°C.

Antibodies and reagents

Antibodies used in this study include rabbit anti-Atg16L1 (PM040; MBL International and CosmoBio), rabbit anti-Atg12 (2010; Cell Signaling Technology), rabbit anti-Atg5 (A0856; Sigma-Aldrich), mouse monoclonal anti-FLAG (clone M2; Sigma-Aldrich), mouse anti-GFP (BD), rabbit antiactin (Sigma-Aldrich), rabbit anti-LC3 for Western blotting (NB100-2220; Novus Biologicals), mouse anti-LC3 for immunofluorescence (clone 5F10; Nanotools), mouse monoclonal anti-Arf6 (clone 3A-1; Santa Cruz Biotechnology, Inc.), rabbit anti-GRAF1 (clone H-73; Santa Cruz Biotechnology, Inc.), rabbit anti-p70S6 kinase (9202; Cell Signaling Technology), rabbit antiphospho-p70S6 kinase (9205; Cell Signaling Technology), mouse monoclonal anti-HA conjugated to FITC (clone HA.11; Covance), mouse monoclonal anti-ARNO (cytohesin-2; ab56510; Abcam), and mouse monoclonal anti-MHC class I conjugated to FITC (clone W6/32; Santa Cruz Biotechnology, Inc.). Reagents used in this study include Baf A1 (Sigma-Aldrich), D-trehalose (D9531; Sigma-Aldrich), rapamycin (Sigma-Aldrich), Alexa Fluor 488– or Alexa Fluor 555–conjugated CTX subunit B (Invitrogen), and transferrin conjugated to Alexa Fluor 488 (Invitrogen).

Plasmids

The pGFP-Arf6 (wild type, Q67L, and N48R; human Arf6 and DKFZp564M0264, inserted into an EGFP background vector; obtained from J.G. Donaldson, National Institutes of Health, Bethesda, MD), pHA-Arf6 (wild type and Q67L; human Arf6 and DKFZp564M0264, inserted into a pcDNA3.1 background vector; obtained from J.G. Donaldson), pFlag-Atg16L1 (the cDNA corresponding to the open reading frame of mouse Apg16L1 was obtained by PCR of IMAGE [Integrated Molecular Analysis of Genomes and their Expression] consortium clone 1480862 and cloned into the p3XFLAG-CMV-10; obtained from R.J. Xavier, Massachusetts General Hospital, Harvard Medical School, Boston, MA), pEGFP-Atg16L1 (the cDNA corresponding to the open reading frame of mouse Apg16L1 cloned into pEGFP-C1; obtained from T. Yoshimori, Research Institute for Microbial Diseases, Osaka University, Osaka, Japan), pmStrawberry-Atg16L1 (the cDNA corresponding to the open reading frame of mouse Apg16L1 cloned into pmStrawberry-C1; obtained from T. Yoshimori), pEGFP-LC3 (microtubule-associated protein 1 light chain 3 β from *Rattus norvegicus* inserted into a EGFP background vector; obtained from T. Yoshimori), pCFP-LC3 (microtubule-associated protein 1 light chain 3 β from *R. norvegicus* inserted into a ECFP background vector; obtained from T. Yoshimori), pEGFP–PLC-δ(PH) (the PH domain from PLC1 cloned into pEGFP-N1; obtained from T. Meyer, Stanford University Medical Center, Stanford, CA), pmStrawberry-Atg4B C74A (the Atg4B cDNA cloned from genomic DNA isolated from MEF cells and inserted into pmStrawberry-C1; the point mutation [C74A] was introduced using the site-directed mutagenesis system [QuikChange; Agilent Technologies]; obtained from T. Yoshimori), pCFP–FKBP12-rapamycin binding (FRB; the N-terminal localization sequence [MLCCMRRTKQVEKNDDDQKI] of the human GAP43 [residues 1–20] was fused to the N terminus of the FRB domain of human mTOR1 [residues 2,019–2,114] amplified from a human EST available from GenBank/EMBL/DDBJ under accession no. AI851671; obtained from P. De Camilli, Yale University School of Medicine, New Haven, CT), pmRFP-FKBP (obtained from P. De Camilli), pmRFP-FKBP-5ase (the human type IV 5ase enzyme, GenBank under accession no. NM_019892, fused to the C terminus of the FKBP; obtained from P. De Camilli), pmRFP-GPi (obtained from B.J. Nichols, Medical Research Council Laboratory of Molecular Biology, Cambridge, England, UK), and pGFP-GRAF1 (wild type and BAR+PH mutant; cDNA constructs encoding human GRAF1 [amino acids 1–759] and GRAF1-BAR+PH [amino acids 1–383] cloned into EGFP-C3; obtained from H.T. McMahon, Medical Research Council Laboratory of Molecular Biology, Cambridge, England, UK) have been previously described elsewhere (Radhakrishna and Donaldson, 1997; Stauffer et al., 1998; Kabeya et al., 2000, 2004; Nichols et al., 2001; Jovanovic et al., 2006; Zoncu et al., 2007; Cadwell et al., 2008; Fujita et al., 2008; Lundmark et al., 2008).

Cell transfection

Cells were seeded at 1–2 × 10^5 per well in 6-well plates, and transfection was performed using Lipofectamine (for DNA) or Lipofectamine 2000 (for siRNA and double transfections with DNA and siRNA; Invitrogen) using the manufacturer's protocol. Predesigned siRNA were ordered from Thermo Fisher Scientific (siRNA IDs: Arf6, ON-TARGETplus SMARTpool L-004008 and single siRNAs from the pool; Cytohesin-2, ON-TARGETplus SMARTpool L-011925; GRAF1, ON-TARGETplus SMARTpool L-008426). Designed siRNA were ordered from Thermo Fisher Scientific (siRNAs: PIP5K, 5′-AUCAUCAAGACCGUCAUGCAC-3′ [Mao et al., 2009]; GRAF1a, 5′-UAUCUCCCAUUCAGCACAGAUAU-3′; GRAF1b, 5′-UUGAAACUGGUACAUCAUGAGUG-3′).

Modulation of autophagy

To inhibit LC3-II degradation, cells were treated with Baf A1 and diluted in cell culture media to a working concentration of 400 nM for 4 h or 200 nM for 16 h, which is saturating for this effect (Sarkar et al., 2007). To induce autophagy in an mTOR-dependent manner, cells were amino acid and serum starved in HBSS (Sigma-Aldrich) for 4 h. To induce autophagy in an mTOR-independent manner, cells were treated with trehalose and diluted in cell culture media to a working concentration of 100 mM for 24 h (Sarkar et al., 2007).

Rapamycin-mediated depletion of PIP_2

Experiments involving rapamycin-mediated recruitment of an inositol 5ase to the plasma membrane were performed as previously described with modifications (Zoncu et al., 2007). The addition of 2.5 µM rapamycin induces the heterodimerization of mRFP-FKBP-5ase to plasma membrane–targeted FRB-CFP, leading to PIP_2 dephosphorylation. For LC3 analysis by Western blotting, cells were treated with 2.5 µM rapamycin for 4 h with or without Baf A1. For immunofluorescence, cells were treated with 2.5 µM rapamycin for 1 h.

CTX internalization assay

Endocytosis was studied using CTX subunit B conjugated to Alexa Fluor 488 or Alexa Fluor 555 as an endocytosis tracer (Ravikumar et al., 2010a). Cells were incubated with 2.5 µg/ml CTX subunit B for 30 min at 37°C, allowing its internalization. Then, cells were fixed and subjected to confocal microscopy analysis.

Endocytosis assay

Endocytosis and recycling assays of transferrin were performed as previously described with modifications (Peden et al., 2004; Puri, 2009). For uptake assays, the cells were grown on 35-mm dishes, serum starved for 1 h, washed twice in PBS/$Ca^{2+}Mg^{2+}$, and incubated with 50 µg/ml transferrin–Alexa Fluor 647 (Invitrogen) at 4°C for 30 min. Cells were then incubated at 37°C for various time intervals in the continuous presence of 20 µg/ml transferrin–Alexa Fluor 647. Cells were then washed, pelleted, and resuspended in 3% paraformaldehyde. Cell-associated transferrin–Alexa Fluor 647 was determined by FACS analysis. For recycling assays, the cells were grown on 35-mm dishes, serum starved for 1 h, washed twice in PBS/$Ca^{2+}Mg^{2+}$, and incubated with transferrin–Alexa Fluor 647 for 30 min at 4°C followed by internalization for 20 min at 37°C in the continuous presence of transferrin–Alexa Fluor 647. Cells were then washed and incubated in complete media supplemented with 100 µg/ml of unlabeled transferrin for various times before fixation. Cell-associated transferrin–Alexa Fluor 647 was determined by FACS analysis. FACS analysis was performed using a flow cytometer (Cytomics FC 500; Beckman Coulter) equipped with 488- and 647-nm lasers, gating for 10,000 transfected (GFP positive) cells, and the amount of internalized transferrin was determined.

Western blotting

Cells were collected, rinsed with PBS, and lysed on ice for 30 min in PBS containing 1% Triton X-100 and complete protease inhibitor cocktail (Roche). Lysates were centrifuged at 15,000 rpm for 5 min at 4°C, and supernatants were resolved by SDS-PAGE and transferred to polyvinylidene

fluoride membranes. The membranes were blocked with TBST (TBS 0.1% and Tween 20) containing 1% nonfat dry milk and were then incubated overnight at room temperature with primary antibodies diluted in TBST. Membranes were washed with TBST, incubated for 1 h at room temperature with 2,500× dilutions of HRP-conjugated secondary antibodies (GE Healthcare) in TBST containing 1% nonfat dry milk, and washed. Immunoreactive bands were then detected using ECL (GE Healthcare).

Fluorescence and immunofluorescence microscopy

For immunofluorescence microscopy, cells were cultured on coverslips, fixed with 4% paraformaldehyde in PBS for 10 min or with ice-cold methanol for 10 min, and permeabilized with 0.1% Triton X-100 in PBS for 5 min. Coverslips were incubated with primary antibodies for 2–24 h, washed three times with PBS, and incubated with secondary antibodies for 60 min. Samples were mounted using antifade reagent with or without DAPI (ProLong Gold; Invitrogen) and observed using a laser confocal microscope (LSM 710; Carl Zeiss). ImageJ (National Institutes of Health) was used to count LC3 dots. BioImage XD was used for the colocalization analysis. 15–20 cells were analyzed for each experiment. Automatic counting of Atg16L1-mStrawberry, Atg16L1-GFP, and LC3 vesicles from HeLa cells stably expressing GFP-mRFP-LC3, endogenous LC3, and endogenous Atg12 was performed using the Cellomics ArrayScan VTI HCS Reader and the Spot Detector BioApplication (Thermo Fisher Scientific).

Statistical analysis

Significance levels for comparisons between groups were determined with *t* tests, repeated measure, or factorial analysis of variance using the StatView software (version 4.53; Abacus Concepts).

Online supplemental material

Fig. S1 shows expression of Arf6 under autophagy stimulation conditions and supplemental quantification data related to Fig. 2. Fig. S2 shows supplemental data related to Fig. 3 on the effect of Arf6 knockdown on autophagosome formation, autophagy substrate degradation, and mTOR activity. Fig. S3 shows the effect of PIP5K on autophagy related to Fig. 4. Fig. S4 shows supplemental data related to Fig. 6 on the role of GRAF1 on autophagy. Fig. S5 shows the effect of autophagy inhibition on endocytosis and recycling of different cargoes. Online supplemental material is available at http://www.jcb.org/cgi/content/full/jcb.201110114/DC1.

We thank Julie G. Donaldson for Arf6 vectors, Tamotsu Yoshimori for LC3, Atg16L1-GFP, Atg16L1-mStrawberry, and Atg4B mutant vectors, Ramnik J. Xavier for the Atg16L1-Flag vector, Ben J. Nichols for GPi vectors, Harvey T. McMahon for GRAF1 vectors, Tobias Meyer for the PLC(PH) vector, and Pietro De Camilli for CFP-FRB, mRFP-FKBP, and mRFP-FKBP-5ase vectors.

We are grateful for funding from a Wellcome Trust Senior and Principal Research Fellowships (to D.C. Rubinsztein) and Cancer Research UK (to C. Puri).

Submitted: 26 October 2011
Accepted: 20 January 2012

References

Brown, F.D., A.L. Rozelle, H.L. Yin, T. Balla, and J.G. Donaldson. 2001. Phosphatidylinositol 4,5-bisphosphate and Arf6-regulated membrane traffic. *J. Cell Biol.* 154:1007–1017. http://dx.doi.org/10.1083/jcb.200103107

Cadwell, K., J.Y. Liu, S.L. Brown, H. Miyoshi, J. Loh, J.K. Lennerz, C. Kishi, W. Kc, J.A. Carrero, S. Hunt, et al. 2008. A key role for autophagy and the autophagy gene Atg16l1 in mouse and human intestinal Paneth cells. *Nature*. 456:259–263. http://dx.doi.org/10.1038/nature07416

Dall'Armi, C., A. Hurtado-Lorenzo, H. Tian, E. Morel, A. Nezu, R.B. Chan, W.H. Yu, K.S. Robinson, O. Yeku, S.A. Small, et al. 2010. The phospholipase D1 pathway modulates macroautophagy. *Nat Commun*. 1:142. http://dx.doi.org/10.1038/ncomms1144

Di Paolo, G., and P. De Camilli. 2006. Phosphoinositides in cell regulation and membrane dynamics. *Nature*. 443:651–657. http://dx.doi.org/10.1038/nature05185

Doherty, G.J., and H.T. McMahon. 2009. Mechanisms of endocytosis. *Annu. Rev. Biochem.* 78:857–902. http://dx.doi.org/10.1146/annurev.biochem.78.081307.110540

Donaldson, J.G. 2003. Multiple roles for Arf6: sorting, structuring, and signaling at the plasma membrane. *J. Biol. Chem.* 278:41573–41576. http://dx.doi.org/10.1074/jbc.R300026200

Donaldson, J.G., N. Porat-Shliom, and L.A. Cohen. 2009. Clathrin-independent endocytosis: a unique platform for cell signaling and PM remodeling. *Cell. Signal.* 21:1–6. http://dx.doi.org/10.1016/j.cellsig.2008.06.020

D'Souza-Schorey, C., and P. Chavrier. 2006. ARF proteins: roles in membrane traffic and beyond. *Nat. Rev. Mol. Cell Biol.* 7:347–358. http://dx.doi.org/10.1038/nrm1910

Fujita, N., M. Hayashi-Nishino, H. Fukumoto, H. Omori, A. Yamamoto, T. Noda, and T. Yoshimori. 2008. An Atg4B mutant hampers the lipidation of LC3 paralogues and causes defects in autophagosome closure. *Mol. Biol. Cell*. 19:4651–4659. http://dx.doi.org/10.1091/mbc.E08-03-0312

Hailey, D.W., A.S. Rambold, P. Satpute-Krishnan, K. Mitra, R. Sougrat, P.K. Kim, and J. Lippincott-Schwartz. 2010. Mitochondria supply membranes for autophagosome biogenesis during starvation. *Cell*. 141:656–667. http://dx.doi.org/10.1016/j.cell.2010.04.009

Hayashi-Nishino, M., N. Fujita, T. Noda, A. Yamaguchi, T. Yoshimori, and A. Yamamoto. 2010. Electron tomography reveals the endoplasmic reticulum as a membrane source for autophagosome formation. *Autophagy*. 6:301–303. http://dx.doi.org/10.4161/auto.6.2.11134

Honda, A., M. Nogami, T. Yokozeki, M. Yamazaki, H. Nakamura, H. Watanabe, K. Kawamoto, K. Nakayama, A.J. Morris, M.A. Frohman, and Y. Kanaho. 1999. Phosphatidylinositol 4-phosphate 5-kinase alpha is a downstream effector of the small G protein ARF6 in membrane ruffle formation. *Cell*. 99:521–532. http://dx.doi.org/10.1016/S0092-8674(00)81540-8

Jovanovic, O.A., F.D. Brown, and J.G. Donaldson. 2006. An effector domain mutant of Arf6 implicates phospholipase D in endosomal membrane recycling. *Mol. Biol. Cell*. 17:327–335. http://dx.doi.org/10.1091/mbc.E05-06-0523

Kabeya, Y., N. Mizushima, T. Ueno, A. Yamamoto, T. Kirisako, T. Noda, E. Kominami, Y. Ohsumi, and T. Yoshimori. 2000. LC3, a mammalian homologue of yeast Apg8p, is localized in autophagosome membranes after processing. *EMBO J.* 19:5720–5728. http://dx.doi.org/10.1093/emboj/19.21.5720

Kabeya, Y., N. Mizushima, A. Yamamoto, S. Oshitani-Okamoto, Y. Ohsumi, and T. Yoshimori. 2004. LC3, GABARAP and GATE16 localize to autophagosomal membrane depending on form-II formation. *J. Cell Sci.* 117:2805–2812. http://dx.doi.org/10.1242/jcs.01131

Kimura, S., T. Noda, and T. Yoshimori. 2007. Dissection of the autophagosome maturation process by a novel reporter protein, tandem fluorescent-tagged LC3. *Autophagy*. 3:452–460.

Klionsky, D.J., H. Abeliovich, P. Agostinis, D.K. Agrawal, G. Aliev, D.S. Askew, M. Baba, E.H. Baehrecke, B.A. Bahr, A. Ballabio, et al. 2008. Guidelines for the use and interpretation of assays for monitoring autophagy in higher eukaryotes. *Autophagy*. 4:151–175.

Kumari, S., and S. Mayor. 2008. ARF1 is directly involved in dynamin-independent endocytosis. *Nat. Cell Biol.* 10:30–41. http://dx.doi.org/10.1038/ncb1666

Lundmark, R., G.J. Doherty, M.T. Howes, K. Cortese, Y. Vallis, R.G. Parton, and H.T. McMahon. 2008. The GTPase-activating protein GRAF1 regulates the CLIC/GEEC endocytic pathway. *Curr. Biol.* 18:1802–1808. http://dx.doi.org/10.1016/j.cub.2008.10.044

Macia, E., F. Luton, M. Partisani, J. Cherfils, P. Chardin, and M. Franco. 2004. The GDP-bound form of Arf6 is located at the plasma membrane. *J. Cell Sci.* 117:2389–2398. http://dx.doi.org/10.1242/jcs.01090

Mao, Y.S., M. Yamaga, X. Zhu, Y. Wei, H.Q. Sun, J. Wang, M. Yun, Y. Wang, G. Di Paolo, M. Bennett, et al. 2009. Essential and unique roles of PIP5K-γ and -α in Fcγ receptor-mediated phagocytosis. *J. Cell Biol.* 184:281–296. http://dx.doi.org/10.1083/jcb.200806121

Mizushima, N., B. Levine, A.M. Cuervo, and D.J. Klionsky. 2008. Autophagy fights disease through cellular self-digestion. *Nature*. 451:1069–1075. http://dx.doi.org/10.1038/nature06639

Moreau, K., B. Ravikumar, M. Renna, C. Puri, and D.C. Rubinsztein. 2011. Autophagosome precursor maturation requires homotypic fusion. *Cell*. 146:303–317. http://dx.doi.org/10.1016/j.cell.2011.06.023

Nichols, B.J., A.K. Kenworthy, R.S. Polishchuk, R. Lodge, T.H. Roberts, K. Hirschberg, R.D. Phair, and J. Lippincott-Schwartz. 2001. Rapid cycling of lipid raft markers between the cell surface and Golgi complex. *J. Cell Biol.* 153:529–541. http://dx.doi.org/10.1083/jcb.153.3.529

Peden, A.A., E. Schonteich, J. Chun, J.R. Junutula, R.H. Scheller, and R. Prekeris. 2004. The RCP-Rab11 complex regulates endocytic protein sorting. *Mol. Biol. Cell.* 15:3530–3541. http://dx.doi.org/10.1091/mbc.E03-12-0918

Puri, C. 2009. Loss of myosin VI no insert isoform (NoI) induces a defect in clathrin-mediated endocytosis and leads to caveolar endocytosis of transferrin receptor. *J. Biol. Chem.* 284:34998–35014. http://dx.doi.org/10.1074/jbc.M109.012328

Radhakrishna, H., and J.G. Donaldson. 1997. ADP-ribosylation factor 6 regulates a novel plasma membrane recycling pathway. *J. Cell Biol.* 139:49–61. http://dx.doi.org/10.1083/jcb.139.1.49

Rameh, L.E., K.F. Tolias, B.C. Duckworth, and L.C. Cantley. 1997. A new pathway for synthesis of phosphatidylinositol-4,5-bisphosphate. *Nature*. 390:192–196. http://dx.doi.org/10.1038/36621

Ravikumar, B., M. Futter, L. Jahreiss, V.I. Korolchuk, M. Lichtenberg, S. Luo, D.C. Massey, F.M. Menzies, U. Narayanan, M. Renna, et al. 2009.

Mammalian macroautophagy at a glance. *J. Cell Sci.* 122:1707–1711. http://dx.doi.org/10.1242/jcs.031773

Ravikumar, B., K. Moreau, L. Jahreiss, C. Puri, and D.C. Rubinsztein. 2010a. Plasma membrane contributes to the formation of pre-autophagosomal structures. *Nat. Cell Biol.* 12:747–757. http://dx.doi.org/10.1038/ncb2078

Ravikumar, B., K. Moreau, and D.C. Rubinsztein. 2010b. Plasma membrane helps autophagosomes grow. *Autophagy*. 6:1184–1186. http://dx.doi.org/10.4161/auto.6.8.13428

Ravikumar, B., S. Sarkar, J.E. Davies, M. Futter, M. Garcia-Arencibia, Z.W. Green-Thompson, M. Jimenez-Sanchez, V.I. Korolchuk, M. Lichtenberg, S. Luo, et al. 2010c. Regulation of mammalian autophagy in physiology and pathophysiology. *Physiol. Rev.* 90:1383–1435. http://dx.doi.org/10.1152/physrev.00030.2009

Rubinsztein, D.C., A.M. Cuervo, B. Ravikumar, S. Sarkar, V. Korolchuk, S. Kaushik, and D.J. Klionsky. 2009. In search of an "autophagomometer". *Autophagy*. 5:585–589. http://dx.doi.org/10.4161/auto.5.5.8823

Sarkar, S., J.E. Davies, Z. Huang, A. Tunnacliffe, and D.C. Rubinsztein. 2007. Trehalose, a novel mTOR-independent autophagy enhancer, accelerates the clearance of mutant huntingtin and alpha-synuclein. *J. Biol. Chem.* 282:5641–5652. http://dx.doi.org/10.1074/jbc.M609532200

Song, J., Z. Khachikian, H. Radhakrishna, and J.G. Donaldson. 1998. Localization of endogenous ARF6 to sites of cortical actin rearrangement and involvement of ARF6 in cell spreading. *J. Cell Sci.* 111:2257–2267.

Stauffer, T.P., S. Ahn, and T. Meyer. 1998. Receptor-induced transient reduction in plasma membrane PtdIns(4,5)P2 concentration monitored in living cells. *Curr. Biol.* 8:343–346. http://dx.doi.org/10.1016/S0960-9822(98)70135-6

van der Vaart, A., J. Griffith, and F. Reggiori. 2010. Exit from the Golgi is required for the expansion of the autophagosomal phagophore in yeast *Saccharomyces cerevisiae*. *Mol. Biol. Cell*. 21:2270–2284. http://dx.doi.org/10.1091/mbc.E09-04-0345

Várnai, P., and T. Balla. 1998. Visualization of phosphoinositides that bind pleckstrin homology domains: calcium- and agonist-induced dynamic changes and relationship to myo-[^{3}H]inositol-labeled phosphoinositide pools. *J. Cell Biol.* 143:501–510. http://dx.doi.org/10.1083/jcb.143.2.501

Várnai, P., B. Thyagarajan, T. Rohacs, and T. Balla. 2006. Rapidly inducible changes in phosphatidylinositol 4,5-bisphosphate levels influence multiple regulatory functions of the lipid in intact living cells. *J. Cell Biol.* 175:377–382. http://dx.doi.org/10.1083/jcb.200607116

Xie, Z., and D.J. Klionsky. 2007. Autophagosome formation: core machinery and adaptations. *Nat. Cell Biol.* 9:1102–1109. http://dx.doi.org/10.1038/ncb1007-1102

Yen, W.L., T. Shintani, U. Nair, Y. Cao, B.C. Richardson, Z. Li, F.M. Hughson, M. Baba, and D.J. Klionsky. 2010. The conserved oligomeric Golgi complex is involved in double-membrane vesicle formation during autophagy. *J. Cell Biol.* 188:101–114. http://dx.doi.org/10.1083/jcb.200904075

Ylä-Anttila, P., H. Vihinen, E. Jokitalo, and E.L. Eskelinen. 2009. 3D tomography reveals connections between the phagophore and endoplasmic reticulum. *Autophagy*. 5:1180–1185. http://dx.doi.org/10.4161/auto.5.8.10274

Zoncu, R., R.M. Perera, R. Sebastian, F. Nakatsu, H. Chen, T. Balla, G. Ayala, D. Toomre, and P.V. De Camilli. 2007. Loss of endocytic clathrin-coated pits upon acute depletion of phosphatidylinositol 4,5-bisphosphate. *Proc. Natl. Acad. Sci. USA*. 104:3793–3798. http://dx.doi.org/10.1073/pnas.0611733104

Zoncu, R., R.M. Perera, D.M. Balkin, M. Pirruccello, D. Toomre, and P. De Camilli. 2009. A phosphoinositide switch controls the maturation and signaling properties of APPL endosomes. *Cell*. 136:1110–1121. http://dx.doi.org/10.1016/j.cell.2009.01.032